Mechanics of Advanced Composite Structures

journal homepage: http://MACS.journals.semnan.ac.ir

Semnan University

A Novel Method for Considering Interlayer Effects between Graphene Nanoribbons and Elastic Medium in Free Vibration Analysis

K. Kamali[a,c], R. Nazemnezhad[b,*]

[a] *School of Mechanical Engineering, Iran University of Science and Technology, Narmak, Tehran, Iran*
[b] *School of Engineering, Damghan University, Damghan, Iran*
[c] *Department of Design, Fateh Sanat Kimia Company, Great Industrial Zone, Shiraz, Iran*

KEYWORDS

Elastic medium
Sandwich theory
Tensile-compressive effects
Shear effects
Euler-Bernoulli theory

ABSTRACT

A complete inspectation on the free vibration of bilayer graphene nanoribbons (BLGNRs) modeled as sandwich beams considered tensile-compressive, and shear effects of van der Waals (vdWs) interactions between adjacent graphene nanoribbons (GNRs) as well as between GNRs and polymer matrix is performed in this research. In this modeling, nanoribbon layers play the role of sandwich beam layers and are modeled based upon the Euler-Bernoulli theory. In order to deliberate effects of vdWs interactions between adjacent GNRs as well as between GNRs and polymer matrix, their equivalent tensile-compressive and shear moduli are contemplated and applied in derivation of governing equations instead of employing conventional Winkler and Pasternak effects for elastic medium. The governing equations of motion are derived by considering the assumptions and employing sandwich beam theory, and natural frequencies are acquired by implementing harmonic differential quadrature method (HDQM). A detailed study is performed to examine the influences of the tensile-compressive and shear effects of vdWs interactions between adjacent GNRs as well as between GNRs and polymer matrix on the free vibration of BLGNRs.

1. Introduction

Graphenes can be synthesized either single-layer or multi-layer. Layers of multi-layer graphenes are located next to each other by weak interactions known as vdWs interactions. These weak interactions change the mechanical and electrical properties of multi-layer graphenes [1], where it can be attributed to the tensile-compressive and shear effects of vdWs interactions. Through an overview of the references studying the mechanical behavior of multilayer graphene sheets (MLGSs) and multilayer graphene nanoribbons (MLGNRs), it is found that they can be classified into two categories. In the first category, only tensile-compressive effects of van der Waals (vdWs) interactions between two graphene layers are contemplated on the mechanical behavior of MLGSs [2-11] or MLGNRs [12-16]. For example, Ansari et al. [17] have explored effects of number of graphene layers and nonlocal parameters by employing Reissner-Mindlin plate theory on the free vibration of MLGSs. In the second category, a handful of researchers have considered only shear effects of vdWs interactions between two graphene layers on the mechanical behavior of MLGNRs [18, 19]. In stance, Liu et al. [20] have explored the bending of cantilever bilayer and trilayer graphene nanoribbons incorporating the interlayer shear through employing Newmark's composite beam theory. They indicate that considering of in-plane displacement of nanoribbons has significant effect on the bending of multilayer graphene nanoribbons. This literature survey reveals that researchers have only considered one of the vdWs interactions effects between GNR layers, the tensile-compressive effect or the shear one. Consequently, as far as it's reported there is no literature investigating the tensile-compressive and shear effects of vdWs interactions between adjacent graphene sheets (GSs) or GNRs, simultaneously.

It is known that in macro dimensions, the tensile-compressive and shear effects of the elastic medium are modeled by Winkler and Pasternak's terms defined in terms of transverse displacement. This approach is also applied in

* Corresponding author. Tel./Fax: +98-23-35220414
E-mail address: rnazemnezhad@du.ac.ir

DOI: 10.22075/MACS.2019.16237.1174
Received 2018-10-19; Received in revised form 2019-05-05; Accepted 2019-06-30

nano dimensions for embedded GSs or GNRs in elastic medium since vdWs interactions are observed not only between adjacent graphene layers but between elastic medium and graphene layers as well [10, 11, 15]. All of these studies have deliberetedonly transverse displacement of graphene layers. In other words, the in-plane displacement of graphene layers has not been considered while it has been mentioned in previous paragraph that considering the in-plane displacement of graphene layers has significant effect on the mechanical behavior of MLGSs and MLGNRs.

From the above consideration, two questions arise. First, what will the tensile-compressive and shear effects of vdWs interactions between adjacent graphene layers be on free vibration of GNRs when they are simultaneously considered? Second, what will the shear effect of elastic medium be on free vibration of GNRs if the in-plane displacement of GNRs is considered? In order to cover the questions, a GNR is modeled based on the sandwich beam theory and tensile-compressive and shear effects of vdWs interactions between adjacent GNRs as well as elastic medium and GNRs are modeled as equivalent tensile-compressive and shear moduli in the equation of motion. The governing equations of motion are derived by applying Hamilton's principle and solved numerically by HDQM. Consequently, natural frequencies are obtained for clamped-clamped boundary conditions. Some comparison studies are performed to indicate the accuracy of formulation and solution procedure. The effects of equivalent tensile-compressive and shear moduli of vdWs interactions between elastic medium and GNRs on the first five natural frequencies of BLGNR are investigated. At last, the effects of equivalent tensile-compressive and shear moduli of vdWs interaction between elastic medium and GNRs on the natural frequencies of BLGNR are numerically compared with those of vdWs interactions between adjacent GNRs.

2. Problem Formulation

If we consider a BLGNR with the surrounding elastic medium in a continuum model as protrayed in Fig. 1, in order to have a better understanding of the study procedure, the flowchart diagram is presented for step by step understanding as Fig. 2. The model consists of five layers: two GNRs, a low density core connecting GNRs to each other (vdWs interactions), and two elastic mediums. Elastic mediums are bonded to the GNRs on the one side and connected to a fixed layer on the other side. All five layers are firmly bonded together, and vdWs interactions inertia is not notable. It is noteworthy to mention that considered elastic mediums are a type of vdWs interactions that connect GNRs to a polymer matrix such as Polyethylene [16]. The Cartesian coordinate system is applied, and the origin is located at the left-hand side of BLGNR in the middle of core thickness. The x and z coordinates of axes are in conformity with the length and thickness of BLGNR, respectively. Here L, b, h_f, h_c and h_e denote length, width, thickness of GNR layers, thickness of core, and thickness of elastic mediums, respectively. The displacement components in accordance with x and z are displayed by u and w, respectively.

The vdWs interactions of elastic mediums are modeled in a way that they can withstand tensile-compressive and shear forces simultaneously. The vdWs interactions between GNR and polymer matrix can be modeled stronger or weaker than vdWs interactions between GNRs with each other. The GNRs are modeled based on Euler-Bernoulli beam theory. According to the theory the displacement field of the upper face (u_t and w_t) and the lower face (u_b and w_b) are defined as following [18].

$$u_t(x,z,t) = u_1(x,t) - \left(z - \frac{h_f + h_c}{2}\right)\frac{\partial w_1}{\partial x} \quad (1)$$

$$w_t(x,z,t) = w_1(x,t) \quad (2)$$

$$u_b(x,z,t) = u_2(x,t) - \left(z + \frac{h_f + h_c}{2}\right)\frac{\partial w_2}{\partial x} \quad (3)$$

$$w_b(x,z,t) = w_2(x,t) \quad (4)$$

in which u_1, w_1 and u_2, w_2 denote the displacements of an arbitrary point on mid-axis of the top and bottom layers, respectively, h_f and h_c are the thickness of the nanoribbon layers and the core, respectively, and z is measured from the $h_c/2$. The strain components of GNRs can be computed as [18]:

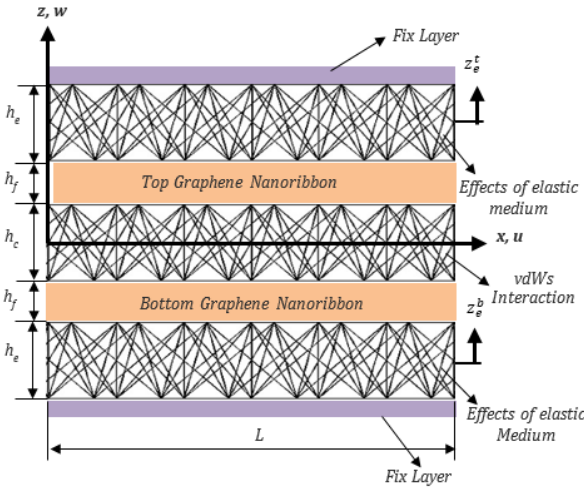

Fig. 1. Geometry and coordinate system of BLGNR embedded in an elastic medium.

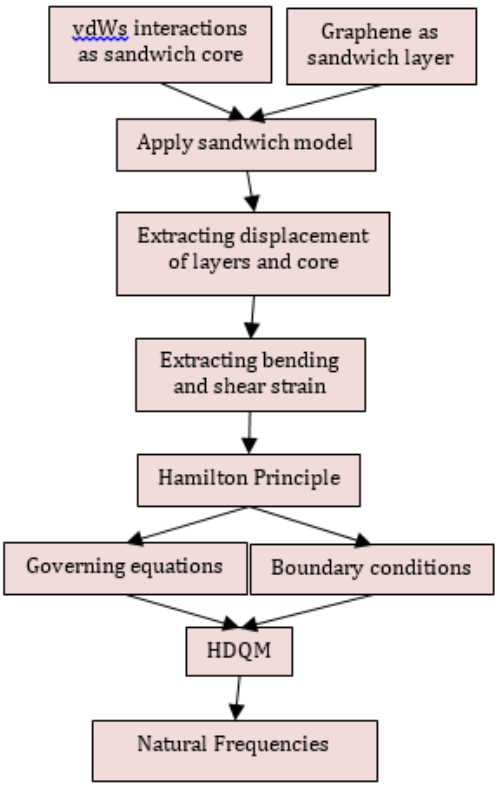

Fig. 2. The flowchart diagram for step by step understanding.

$$\varepsilon_{xx}^{t} = \frac{\partial u_t}{\partial x} = \frac{\partial u_1}{\partial x} - \left(z - \frac{h_f + h_c}{2}\right)\frac{\partial^2 w_1}{\partial x^2} \tag{5}$$

$$\varepsilon_{xx}^{b} = \frac{\partial u_b}{\partial x} = \frac{\partial u_2}{\partial x} - \left(z + \frac{h_f + h_c}{2}\right)\frac{\partial^2 w_2}{\partial x^2} \tag{6}$$

weher ε_{xx}^{t} and ε_{xx}^{b} are the strain components of the top and bottom layers of graphene nanoribbon, respectively.

Pursuant to thesandwich beam theory, the longitudinal and transverse displacements (u_c and w_c) of the core (vdWs interaction between GNRs) are assumed linear through its thickness. On that account, the displacement components of the core can be obtained as following [18]:

$$u_c(x,y,z) = \left[\frac{u_1 - u_2}{2} + \frac{h_f}{4}\left(\frac{\partial w_1}{\partial x} + \frac{\partial w_2}{\partial x}\right)\right]\frac{2z}{h_c} + \left[\frac{u_1 + u_2}{2} + \frac{h_f}{4}\left(\frac{\partial w_1}{\partial x} - \frac{\partial w_2}{\partial x}\right)\right] \tag{7}$$

$$w_c(x,y,z) = (w_1 - w_2)\frac{z}{h_c} + \left(\frac{w_1 + w_2}{2}\right) \tag{8}$$

As a general method, the elastic mediums are modeled as Winkler or Pasternak foundation [10, 11, 21, 22]. Winkler foundation considers only normal pressure, while the Pasternak foundation describes not only normal pressure but transverse shear stress as well. On the contrary to the conventional, the authors present a new model that contemplated the tensile-compressive and shear effects of the elastic medium for the first time. The modeling is based on the sandwich theory, and it is assumed that elastic medium has specific thickness, and longitudinal and transverse displacements of the elastic medium are varied linearly through the elastic medium thickness. Since the elastic medium is vdWs interactions between fixed matrix and GNRs, the displacement equations of the elastic medium can be acquired as below:

$$u_e^t = \left(\frac{1}{2} - \frac{z_e^t}{h_e}\right)\left(u_1 - \frac{h_f}{2}\frac{\partial w_1}{\partial x}\right) \tag{9}$$

$$w_e^t = \left(\frac{1}{2} - \frac{z_e^t}{h_e}\right)w_1 \tag{10}$$

$$u_e^b = \left(\frac{1}{2} - \frac{z_e^b}{h_e}\right)\left(u_2 + \frac{h_f}{2}\frac{\partial w_2}{\partial x}\right) \tag{11}$$

$$w_e^b = \left(\frac{1}{2} + \frac{z_e^b}{h_e}\right)w_2 \tag{12}$$

in which u_e^t, w_e^t and u_e^b, w_e^b denote the displacements of the top and bottom elastic mediums, h_e is the elastic medium thickness, and z_e^b and z_e^t are measured from the $h_e/2$. Since the core and elastic mediums are considered not to resist in-plane loading, their longitudinal strains are insignificant. While bending and shear strains of the core (ε_{zz}^{c} and γ_{xz}^{c}) and elastic mediums ($\varepsilon_{zz}^{e,t}.\varepsilon_{zz}^{e,b}.\gamma_{xz}^{e,t}.$ and $\gamma_{xz}^{e,b}$) are significant and expressed as follow:

$$\varepsilon_{zz}^{c} = \frac{\partial w_c}{\partial z} = \frac{w_1 - w_2}{h_c} \tag{13}$$

$$\gamma_{xz}^{c} = \frac{\partial u_c}{\partial z} + \frac{\partial w_c}{\partial x} = \left[\frac{u_1 - u_2}{2} + \frac{h_f}{4}\left(\frac{\partial w_1}{\partial x} + \frac{\partial w_2}{\partial x}\right)\right]\frac{2}{h_c} + \left(\frac{\partial w_1}{\partial x} - \frac{\partial w_2}{\partial x}\right)\frac{z}{h_c} + \frac{1}{2}\left(\frac{\partial w_1}{\partial x} + \frac{\partial w_2}{\partial x}\right) \tag{14}$$

$$\varepsilon_{zz}^{e,t} = \frac{\partial w_e^t}{\partial z_e^t} = -\frac{w_1}{h_e} \tag{15}$$

$$\varepsilon_{zz}^{e,b} = \frac{\partial w_e^b}{\partial z_e^b} = \frac{w_2}{h_e} \tag{16}$$

$$\gamma_{xz}^{e,t} = \frac{\partial u_e^t}{\partial z_e^t} + \frac{\partial w_e^t}{\partial x} = \frac{\left(\frac{h_f}{2}\frac{\partial w_1}{\partial x} - u_1\right)}{h_e} + \left(\frac{1}{2} - \frac{z_e^t}{h_e}\right)\frac{\partial w_1}{\partial x} \tag{17}$$

$$\gamma_{xz}^{e,b} = \frac{\partial u_e^b}{\partial z_e^b} + \frac{\partial w_e^b}{\partial x} = \frac{\left(\frac{h_f}{2}\frac{\partial w_2}{\partial x} + u_2\right)}{h_e} + \left(\frac{1}{2} + \frac{z_e^b}{h_e}\right)\frac{\partial w_2}{\partial x} \tag{18}$$

Now the stress-strain relations for the core, two faces, and two elastic mediums can be acquired as

$$\sigma_{xx}^{k} = E_f \varepsilon_{xx}^{k}\,; \qquad k = t,b \tag{19}$$

$$\sigma_{zz}^{c} = E_c \varepsilon_{zz}^{c}\,; \qquad \tau_{xz}^{c} = G_c \gamma_{xz}^{c} \tag{20}$$

$$\sigma_{xx}^{e,k} = E_e \varepsilon_{xx}^{e,k}\,; \qquad \tau_{xz}^{e,k} = G_e \gamma_{xz}^{e,k}\,;\ k = t,b \tag{21}$$

where E_f, E_c, G_c, E_e and G_e are the elastic modulus of a single layer of GNR, tensile-compressive modulus of the core, shear modulus of the core, tensile-compressive modulus of the elastic medium, and shear modulus of the elastic medium, respectively, σ_{xx} and σ_{zz} are the normal stresses in the *x* and *z* directions, respectively, and τ_{xz} is the shear stress in the *xz* plane.

By employing Hamilton's principle (equation (22)). Where U and T are potential energy and kinetic energy, and t is as time. δu and δT are defined as equation (23-26).

$$\int_{t1}^{t2} (\delta_u - \delta_t)\, dt = 0 \tag{22}$$

$$\begin{aligned}\delta u_1 :& -E_f A_f \frac{\partial^2 u_1}{\partial x^2} + \left(\frac{G_c A_c}{h_c^2} + \frac{G_e A_e}{h_e^2}\right) u_1 - \\ & \left(\frac{G_c A_c}{h_c^2}\right) u_2 + \left(\frac{G_c A_c (h_f + h_c)}{2h_c^2}\right)\frac{\partial w_2}{\partial x} + \\ & \left(\frac{G_c A_c (h_f + h_c)}{2h_c^2} - \frac{G_e A_e (h_f + h_e)}{2h_e^2}\right)\frac{\partial w_1}{\partial x} \\ & + \rho A_f \frac{\partial^2 u_1}{\partial t^2} = 0\end{aligned} \tag{23}$$

$$\begin{aligned}\delta u_2 :& -E_f A_f \frac{\partial^2 u_2}{\partial x^2} - \left(\frac{G_c A_c}{h_c^2}\right) u_1 + \\ & \left(\frac{G_c A_c}{h_c^2} + \frac{G_e A_e}{h_e^2}\right) u_2 - \left(\frac{G_c A_c (h_f + h_c)}{2h_c^2}\right)\frac{\partial w_1}{\partial x} \\ & - \\ & \left(\frac{G_c A_c (h_f + h_c)}{2h_c^2} - \frac{G_e A_e (h_f + h_e)}{2h_e^2}\right)\frac{\partial w_2}{\partial x} \\ & + \rho A_f \frac{\partial^2 u_2}{\partial t^2} = 0\end{aligned} \tag{24}$$

$$\begin{aligned}\delta w_1 :& E_f I_f \frac{\partial^4 w_1}{\partial x^4} - \\ & \left(\frac{G_c A_c (h_f + h_c)}{2h_c^2} - \frac{G_e A_e (h_f + h_e)}{2h_e^2}\right)\frac{\partial u_1}{\partial x} \\ & + \left(\frac{G_c A_c (h_f + h_c)}{2h_c^2}\right)\frac{\partial u_2}{\partial x} - \\ & \left(\frac{G_c A_c (h_f + h_c)^2}{4h_c^2} - \frac{G_c I_c}{h_c^2}\right)\frac{\partial^2 w_2}{\partial x^2} - \\ & \left(\frac{G_c A_c (h_f + h_c)^2}{4h_c^2} + \frac{G_c I_c}{h_c^2} + \frac{G_e A_e (h_f + h_e)^2}{4h_e^2} \right. \\ & \left. + \frac{G_e I_e}{h_e^2}\right)\frac{\partial^2 w_1}{\partial x^2} + \\ & \left(\frac{E_c A_c}{h_c^2} + \frac{E_e A_e}{h_e^2}\right) w_1 - \left(\frac{E_c A_c}{h_c^2}\right) w_2 + \rho A_f \frac{\partial^2 w_1}{\partial t^2} \\ & = 0\end{aligned} \tag{25}$$

$$\begin{aligned}\delta w_2 :& E_f I_f \frac{\partial^4 w_2}{\partial x^4} - \left(\frac{G_c A_c (h_f + h_c)}{2h_c^2}\right)\frac{\partial u_1}{\partial x} + \\ & \left(\frac{G_c A_c (h_f + h_c)}{2h_c^2} - \frac{G_e A_e (h_f + h_e)}{2h_e^2}\right)\frac{\partial u_2}{\partial x} - \\ & \left(\frac{G_c A_c (h_f + h_c)^2}{4h_c^2} + \frac{G_c I_c}{h_c^2} + \frac{G_e A_e (h_f + h_e)^2}{4h_e^2} \right. \\ & \left. + \frac{G_e I_e}{h_e^2}\right)\frac{\partial^2 w_2}{\partial x^2} - \\ & \left(\frac{G_c A_c (h_f + h_c)^2}{4h_c^2} - \frac{G_c I_c}{h_c^2}\right)\frac{\partial^2 w_1}{\partial x^2} - \left(\frac{E_c A_c}{h_c^2}\right) w_1 \\ & + \\ & \left(\frac{E_c A_c}{h_c^2} + \frac{E_e A_e}{h_e^2}\right) w_2 + \rho A_f \frac{\partial^2 w_2}{\partial t^2} = 0\end{aligned} \tag{26}$$

where A_f, A_c and A_e are the cross sectional area of the faces, the core, and the elastic mediums , respectively. Furthermore, I_f, I_c and I_e are second moment of area of the faces, the core, and the elastic mediums, respectively, and ρ is density of graphene nanoribbons. The developed coupled equations (equations (23)-(26)) are the governing equations of motion in which their couplings are as results to the tensile-compressive and shear effects of vdWs interactions between carbon-carbon atoms as well as vdWs interactions between nanoribbons and polymer matrix. Confirming to Hamilton's principle the boundary conditions are also generated as follow:

$$\delta u_1 : E_f A_f \frac{\partial u_1}{\partial x} = 0 \tag{27}$$

$$\delta u_2 : E_f A_f \frac{\partial u_2}{\partial x} = 0 \tag{28}$$

$$\begin{aligned}\delta w_1 :& -E_f I_f \frac{\partial^3 w_1}{\partial x^3} + \\ & \left(\frac{G_c A_c (h_f + h_c)}{2h_c^2} - \frac{G_e A_e (h_f + h_e)}{2h_e^2}\right) u_1 - \\ & \left(\frac{G_c A_c (h_f + h_c)}{2h_c^2}\right) u_2 + \\ & \left(\frac{G_c A_c (h_f + h_c)^2}{4h_c^2} + \frac{G_c I_c}{h_c^2} + \frac{G_e A_e (h_f + h_e)^2}{4h_e^2} \right. \\ & \left. + \frac{G_e I_e}{h_e^2}\right)\frac{\partial w_1}{\partial x} +\end{aligned} \tag{29}$$

$$\left(\frac{G_c A_c\left(h_f+h_c\right)^2}{4h_c^2}-\frac{G_c I_c}{h_c^2}\right)\frac{\partial w_2}{\partial x}=0$$

$$\delta w_2: -E_f I_f\frac{\partial^3 w_2}{\partial x^3}+\left(\frac{G_c A_c\left(h_f+h_c\right)}{2h_c^2}\right)u_1-\left(\frac{G_c A_c\left(h_f+h_c\right)}{2h_c^2}-\frac{G_e A_e\left(h_f+h_e\right)}{2h_e^2}\right)u_2+\left(\frac{G_c A_c\left(h_f+h_c\right)^2}{4h_c^2}-\frac{G_c I_c}{h_c^2}\right)\frac{\partial w_1}{\partial x}+\left(\frac{G_c A_c\left(h_f+h_c\right)^2}{4h_c^2}+\frac{G_c I_c}{h_c^2}+\frac{G_e A_e\left(h_f+h_e\right)^2}{4h_e^2}+\frac{G_e I_e}{h_e^2}\right)\frac{\partial w_2}{\partial x}=0 \quad (30)$$

$$\frac{\partial}{\partial x}(\delta w_1): E_f I_f\frac{\partial^2 w_1}{\partial x^2}=0 \quad (31)$$

$$\frac{\partial}{\partial x}(\delta w_2): E_f I_f\frac{\partial^2 w_2}{\partial x^2}=0 \quad (32)$$

In the present work, a BLGNR with clamp-clamp ends is inspected where equations of the boundary condition are presented as follow:

$$u_1=u_2=w_1=w_2=\frac{\partial w_1}{\partial x}=\frac{\partial w_2}{\partial x}=0 \quad (33)$$

2.1. Solution Procedure

Because of the coupling of the governing equations of motion (equations (23)-(26)), the problem does not have an analytical or semi-analytical solution. For this reason, HDQM [18] is employed. This method was initiated from the idea of conventional integral quadrature and is a numerical discretization technique for the approximation of derivatives [23, 24]. Following this idea, the *n*th order derivative of the function *f(x)* with *N* grid points, is approximated by a linear sum of all the functional values in the entire domain, that is,

$$\frac{\partial^n}{\partial x^n}f(x_i)=\sum_{j=1}^{N}A_{ij}^{(n)}.f\left(x_j\right),\qquad i=1,2,\dots,N \quad (34)$$

where $f\left(x_j\right)$ represents the functional value at a grid point x_j, and $A_{ij}^{(n)}$ is the weighting coefficient of the *n*th order derivative. In order to generate a mesh in x coordinate on the computational domain of BLGNR ($0\le x\le L$), Chebyshev distribution method is involved, which is described as follow:

$$x_i=\frac{L}{2}\left[1-\cos\left(\frac{i-1}{N-1}\pi\right)\right];\ \ i=1,2,\dots,N \quad (35)$$

For free vibration analysis of BLGNRs, the dynamic displacement vectors are expressed as follow:

$$\{u_i(x,t),w_i(x,t)\}=\{U_i(x),W_i(x)\}e^{j\omega t};\ \ i=1,2 \quad (36)$$

where ω is the natural frequency of BLGNR. By substituting equation (37) into equations (23)-(26) and (27)-(32), using $X=\frac{x}{L}$, $\overline{U}_i=\frac{U_i}{h}$ and $\overline{W}_i=\frac{W_i}{h}$ as dimensionless parameters, where h is a carbon atom thickness, and implementing HDQM, the governing equations and boundary conditions are discretized. In order to avoid repetitive representations, only the discretized form of equation (25) is presented here, as follows:

$$\begin{aligned}&\frac{G_c A_c h^2}{E_f A_f h_c^2}\Bigg\{\frac{I_c}{L^2 A_c}\left[\sum_{k=1}^{N}A_{ik}^{(2)}\overline{W}_2(X_k)-\sum_{k=1}^{N}A_{ik}^{(2)}\overline{W}_1(X_k)\right]-\left(\frac{h_f+h_c}{2L}\right)^2\left[\sum_{k=1}^{N}A_{ik}^{(2)}\overline{W}_2(X_k)+\sum_{k=1}^{N}A_{ik}^{(2)}\overline{W}_1(X_k)\right]+\frac{h_f+h_c}{2L}\left[\sum_{k=1}^{N}A_{ik}^{(1)}\overline{U}_2(X_k)-\sum_{k=1}^{N}A_{ik}^{(1)}\overline{U}_1(X_k)\right]\Bigg\}\\&+\frac{G_e A_e h^2\left(h_f+h_e\right)}{2E_f A_f L h_e^2}\sum_{k=1}^{N}A_{ik}^{(1)}\overline{U}_1(X_k)-\frac{G_e\left[A_e\left(h_f+h_e\right)^2+4I_e\right]h^2}{4E_f A_f L^2 h_e^2}\sum_{k=1}^{N}A_{ik}^{(2)}\overline{W}_1(X_k)+\frac{h^2 I_f}{A_f L^4}\sum_{k=1}^{N}A_{ik}^{(4)}\overline{W}_1(X_k)+\\&\frac{E_c A_c h^2}{E_f A_f h_c^2}\left(\overline{W}_1(X_i)-\overline{W}_2(X_i)\right)+\frac{E_e A_e h^2}{E_f A_f h_e^2}\overline{W}_1(X_i)=\frac{\rho h^2\omega^2}{E_f}\overline{W}_1(X_i)\end{aligned} \quad (37)$$

Writing boundary condition and governing equations in matrix form yields the following equations

$$[A_{BB}]\{W_B\}+[A_{BI}]\{W_I\}=0 \quad (38)$$

$$[A_{IB}]\{W_B\}+[A_{II}]\{W_I\}=\omega^2\{W_I\} \quad (39)$$

where $\{W_B\}$ and $\{W_I\}$ are the functional values of the boundary and interior points, respectively. After mathematical simplifications on equations (38) and (39), the following final eigenvalue equation system can be acquired:

$$\left[[A_{II}] - [A_{IB}][A_{BB}]^{-1}[A_{BI}]\right]\{W_I\} = \omega^2\{W_I\} \qquad (40)$$

Now, the natural frequencies and corresponding mode shapes of BLGNRs can be obtained by solving equation (40).

3. Results and Discussion

In order to study tensile-compressive and shear effects of the elastic medium on the natural frequencies of BLGNRs the bending rigidity, mass density, length, thickness of sandwich core, width and thickness of nanoribbon layers are considered to be, respectively: $D_b = 2.4$ eV, $\rho = 2260$ kg. m^{-3}, $L = 10$ nm, $h_c = 0.335$ nm, $b = 2$ nm and $h_f = 0.335$ nm. Moreover, the equivalent tensile-compressive and shear (in armchair direction) moduli of vdWs interactions between two GNR layers are taken 26.6 GPa, and 482 MPa, respectively [1], and the following parameters are defined

$$E^* = \frac{E_e}{E_c} \qquad G^* = \frac{G_e}{G_c} \qquad (41)$$

The definitions of E^* and G^* say that vdWs interactions between polymer matrix and GNR will be stiffer than those between GNR layers if E^* and $G^* > 1$; and it is the other way round if E^* and $G^* < 1$. It is important to note that E_c and G_c are constant in the above definitions.

3.1. Comparison studies

In this section, two comparison studies for natural frequencies are conducted in Tables 1 and 2 to validate the results of the present formulation and confirm its reliability. As the first comparison study, in Table 1 results of the present formulation are compared with the first and second natural frequencies of a CBLGNR with only contempalting the shear modulus effect of vdWs interactions between GNR layers (the tensile-compressive modulus is considered to be high enough, $E_c = 4$ TPa) [18].In the second comparison study (see Table 2) the present results are compared with the out-of-plane/in-phase (OPl-IPh) and out-of-plane/anti-phase (OPl-APh) natural frequencies of a simply supported double nano-beam [15] with deliberating only the tensile-compressive modulus effect of vdWs interactions of GNRs (the shear modulus of vdWs interactions between GNRs is considered to be zero, $G_c = 0$) for three different values of the tensile-compressive modulus. As it can be observed from Tables 1 and 2, the results of the present study are in excellent agreement with those reported in literatures.

3.2. Benchmark Results

In order to inspect the tensile-compressive and shear effects of a surrounding elastic medium on the vibrational behavior of BLGNRs, numerical natural frequency results for different $E^*$and G^* values are given. To this end, the frequency ratio is defined as follow:

$$\text{Frequency ratio} = \frac{\text{Frequency of BLGNR with elastic medium}}{\text{Frequency of BLGNR without elastic medium}}$$

Plus, five natural frequencies of BLGNR without elastic medium are presented in Table 3. The natural frequencies of BLGNR with elastic medium can be computed by applying Table 3 and frequency ratio values.

In the following, results are presented in three sections. In the first section, only tensile-compressive effects and in the second section only shear effects of vdWs interactions of the elastic medium on the first five natural frequencies of BLGNR are investigated.

In the third section, the tensile-compressive and shear effects of vdWs interactions of the elastic medium on natural frequencies are simultaneously explored. Addintionally, in the last section, effects of aspect ratio of BLGNRs on the natural frequencies is contemplated for two different values of elastic medium moduli.

Firstly, in Fig. 3 variations of frequency ratio versus the mode number are plotted for various values of E^* ($0.001 < E^* < 10$ or $0.0266 < \mathrm{E}_e < 266$ GPa). It is noteworthy to mention that in Fig. 3 the value of G^* is set to zero.

Table 1. Comparison of first and second natural frequencies of CBLGNR incorporating the shear modulus effect of vdWs interactions of GNR layers ($E_c = 4$ TPa) and $D_b = 1.4$ eV.

Shear modulus (GPa)	1st frequency (GHz)		2nd frequency (GHz)	
	Ref. [18]	Present study	Ref. [18]	Present study
0.25	6.324	6.324	29.360	29.360
4.6	10.246	10.246	62.591	63.591

Table 2. Comparison of OPl-IPh and OPl-APh dimensionless natural frequencies of BLGNR ($G_c = 0$).

Tensile-compressive modulus (GPa)	First OPl-IPl frequency		First OPl-APh frequency	
	Ref. [15]	Present study	Ref. [15]	Present study
10	9.869	9.869	1220	1220
20	9.869	9.869	1725.4	1725.4
30	9.869	9.869	2113.1	2113.1

It is observed from Fig. 3 that all frequency ratio curves indicate a monotonically reducing trend as the mode number increases. This implies that the tensile-compressive effects of the elastic medium on natural frequencies decrease by increasing the mode number. Furthermore, Fig. 3 shows that the tensile-compressive effects of elastic medium are notably less influential at higher mode numbers. This is a result of this fact that as the mode number increases, the dominant displacement of BLGNR layers changes from out of plane to in-plane. In general, it can also be observed in Fig. 3 that lower mode numbers are more dependent on the variations of the tensile-compressive modulus value than higher ones. Furthermore, Fig. 3 displays that the first five natural frequencies of BLGNRs are independent of the value of tensile-compressive modulus for $E^* \geq 0.5$. The reason of this is that increasing the value of E^* causes the elastic medium to become stiffer, and accordingly, displacements of BLGNR layers become completely in-plane. As a final point it is worth noting that since by increasing the tensile-compressive modulus of elastic medium displacements of BLGNR layers become completely in-plane, it is expected that natural frequencies of BLGNRs become independent of the value of interlayer tensile-compressive modulus as well.

Continously, in order to consider the shear modulus effects of the elastic medium on the natural frequencies of BLGNRs, Fig. 4 is plotted. In Fig. 4 variations of frequency ratios versus mode number are inidacted for various values of G^* ($0.01 \leq G^* \leq 100$ or $0.00482 \leq G_e \leq 48.5$ GPa) when $E^* = 0.001$. Fig. 4 shows that all frequency ratio curves have a monotonically decreasing trend as the mode number increases, like the one observed in Fig. 3. Consequently, an important result is that the shear effects of the elastic medium on the natural frequencies decrease by increasing the mode number.

Unlike Fig. 3 where variations of the frequency ratios versus the mode number are different for various values of the E^*, it can be observed from Fig. 4 that variations of the frequency ratios versus the mode number are the same for various values of the G^*. Furthermore, it can be observed from Fig. 4 that by increasing the mode number, variations of the frequency ratios become independent of values of the shear modulus of the elastic medium if $G^* \leq 1$. In another words, effects of the interlayer shear modulus on frequency ratios become more pronounced for $G^* > 1$. A final point to mention is that since by increasing the shear modulus of the elastic medium displacements of BLGNR layers become completely out of plane, it is expected that the natural frequencies of BLGNRs also become independent of the value of the interlayer shear modulus.

After deliberating tensile-compressive and shear moduli effects of the elastic medium on the frequency ratios of BLGNRs separately, now ispecting their effects are simultaneously desired. To this end, variations of the frequency ratios versus the mode number for various values of E^* and G^* are protrayed in Fig. 5. It is seen from Fig. 5 that the tensile-compressive and shear moduli effects of the elastic medium have a significant influence on low mode numbers, and their effects decrease by increasing the mode numbers. Also, as the stiffness of the elastic medium increases (increasing E^* and G^*), the frequency ratio incrases. This implies that the natural frequencies of the embedded bilayer nanoribbons will increase by increasing E^* and G^*. The final point of Fig. 5 is that for low values of the E^* and G^*, variations of the frequency ratios are independent of the mode number.

Table 3. Natural frequencies of BLGNR without elastic medium.

Mode number	ω_1	ω_2	ω_3	ω_4	ω_5
Frequency (GHz)	40.61	92.94	163.42	252.01	347.90

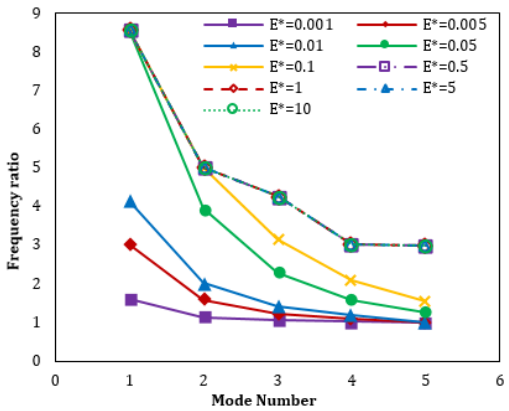

Fig. 3. Variations of frequency ratio with mode number for different values of E^*

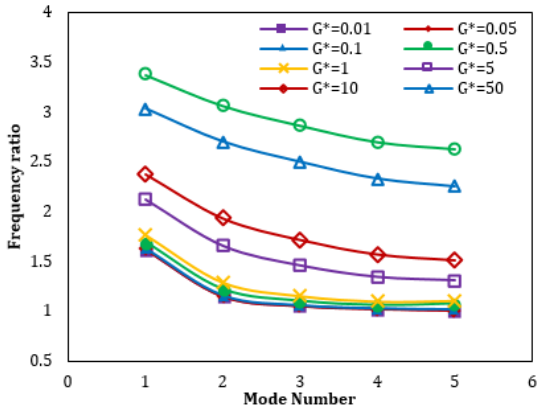

Fig. 4. Variations of frequency ratio with mode number for different values of G^*

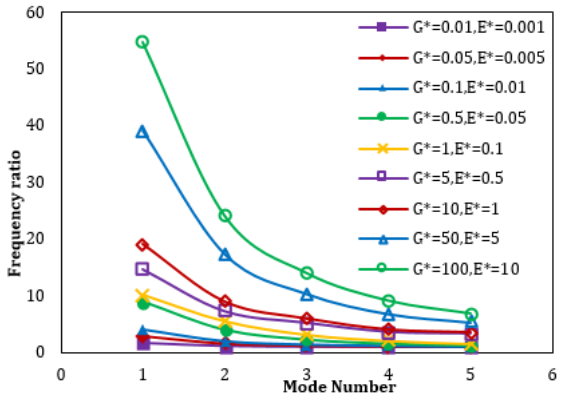

Fig. 5. Variations of frequency ratio versus mode number for various values of E^* and G^*

Comparing Fig. 5 with Figs. 3 and 4 represent that when both the tensile-compressive and shear moduli of elastic medium are simultaneously considered, their effects on natural frequencies significantly increase in comparison with the case that their effects are separately investigated. For example, when $E^* = 10$ and $G^* = 0$, the first frequency ratio becomes 8.57; and when $E^* = 0.001$ and $G^* = 100$, the first frequency ratio becomes 3.38. But when $E^* = 10$ and $G^* = 100$, the first frequency ratio reaches to 54.65. At last, in Tables 4 and 5, influences of the tensile-compressive and shear moduli of elastic medium are numerically compared with those of interlayer vdWs interactions. In Tables 4 and 5, natural frequencies and their value changes are categorized as a result of considering the elastic medium and interlayer vdWs moduli, respectively. The following findings can be highlighted by comparing the results shown in Tables 4 and 5:

Table 4. Frequency value and change in frequency value for three different cases of tensile-compressive and shear moduli of elastic medium (E_c = 26.6 GPa, G_c = 0.482 GPa).

Mode number	E^*=0.01 G^*=0	E^*=0.05 G^*=0	Change in frequency value (%)	E^*=0.001 G^*=0.1	E^*=0.001 G^*=0.5	Change in frequency value (%)	E^*=0.01 G^*=0.1	E^*=0.05 G^*=0.5	Change in frequency value (%)
	Frequency (GHz)			Frequency (GHz)			Frequency (GHz)		
1	167.94	347.90	107.15	66.29	68.81	3.80	168.21	367.26	118.33
2	187.50	366.63	95.54	107.79	113.52	5.31	188.39	377.95	100.62
3	230.76	375.42	62.68	173.22	180.38	4.13	232.16	380.93	64.08
4	300.07	399.27	33.06	259.32	267.44	3.13	301.88	403.30	33.60
5	347.90	442.39	27.16	354.75	375.02	5.71	354.75	448.90	26.54
6	395.55	467.65	18.23	366.32	380.93	3.99	397.60	491.83	23.70
7	466.46	512.51	9.87	471.33	491.15	4.21	471.55	520.36	10.35
8	515.70	609.98	18.28	494.44	503.57	1.85	517.90	619.21	19.56
9	658.75	695.81	5.63	642.75	652.18	1.47	661.07	712.89	7.84
10	695.81	734.71	5.59	699.26	712.89	1.95	699.26	745.20	6.57
11	762.32	762.69	0.05	765.40	777.72	1.61	765.43	777.91	1.63
12	824.68	886.75	7.53	812.49	822.13	1.19	827.07	897.80	8.55
13	1012.63	1043.71	3.07	1003.23	1013.02	0.98	1015.07	1055.17	3.95
14	1043.71	1063.80	1.92	1046.02	1055.17	0.88	1046.02	1075.35	2.80
15	1089.15	1089.20	0.00	1091.32	1100.01	0.80	1091.33	1100.04	0.80

Table 5. Frequency value and change in frequency value for three different cases of tensile-compressive and shear moduli of core (E^* = 0, G^* = 0).

Mode number	E_c=26.6 G_c=0	E_c=42 G_c=0	Change in frequency value (%)	E_c=4000 G_c=0.482	E_c=4000 G_c=4.8	Change in frequency value (%)	E_c=26.6 G_c=0.482	E_c=42 G_c=4.8	Change in frequency value (%)
	Frequency (GHz)			Frequency (GHz)			Frequency (GHz)		
1	23.96	23.96	0.00	40.61	69.95	72.25	40.61	69.95	72.25
2	66.05	66.05	0.00	92.94	164.77	77.28	92.94	164.77	77.28
3	129.48	129.48	0.00	163.42	282.98	73.16	163.42	282.98	73.16
4	214.04	214.04	0.00	252.01	347.90	38.05	252.01	347.90	38.05
5	319.73	319.73	0.00	347.90	417.09	19.89	347.90	417.09	19.89
6	347.90	347.90	0.00	360.43	565.43	56.88	360.43	565.43	56.88
7	347.90	347.90	0.00	466.20	695.81	49.25	466.20	695.81	49.25
8	446.57	446.57	0.00	489.46	727.67	48.67	489.46	727.67	48.67
9	594.55	594.55	0.00	638.29	904.78	41.75	638.29	904.78	41.75
10	695.81	695.81	0.00	695.81	1041.59	49.69	695.81	1041.59	49.69
11	695.81	695.81	0.00	762.29	1043.71	36.92	762.29	1043.71	36.92
12	763.66	763.66	0.00	808.42	1099.87	36.05	808.42	1099.87	36.05
13	953.92	953.92	0.00	999.43	1209.79	21.05	999.43	1209.79	21.05
14	1043.71	1043.71	0.00	1043.71	1311.14	25.62	1043.71	1311.14	25.62
15	1043.71	1043.71	0.00	1089.14	1391.62	27.77	1089.14	1391.62	27.77

- The tensile-compressive modulus of the elastic medium has a significant influence on the low mode numbers, and its effects become less by increasing the mode numbers whereas the interlayer tensile-compressive modulus of vdWs interactions does not have any effects on low mode numbers, and at higher mode numbers its influence increases as the mode number increases.
- At low mode numbers, the influences of the tensile-compressive modulus of the elastic medium are more than those of the shear modulus of the elastic medium while there is no sensible difference between their influences at higher mode numbers. However, the interlayer tensile-compressive modulus of vdWs interactions does not have any effects on low mode numbers, and its influence is more than the interlayer shear modulus at high mode numbers.
- The major influences of both the interlayer shear modulus and the shear modulus of the elastic medium are at low mode numbers, and their effects decrease as the mode number increases.
- When both the tensile-compressive and shear modulus effects are simultaneously deliberated, their influences become more in comparison with the cases that they are separately considered. This is true for both the elastic medium and interlayer vdWs interactions moduli.
- However, the interlayer moduli of vdWs interactions have the highest effects on natural frequencies at low and very high mode numbers, although it can be observed that they have noticible influence on other natural frequencies between the low and very high mode numbers. Whereas the elastic medium moduli effects are only pronounced at low mode numbers.

4. Conclusions

The tensile-compressive and shear effects of vdWs interactions between adjacent GNRs as well as elastic medium and GNRs on free vibration of BGNRs are investigated. In order to explore in-plane displacements of GNRs and both tensile-compressive and shear effects of vdWs interactions, sandwich beam theory is utilized. Governing equations of motion are acquired and solved numerically by HDQM. Results show that lower mode numbers are more dependent on the tensile-compressive effects of the elastic medium than higher ones. Furthermore, the tensile-compressive effects of elastic medium on natural frequencies are more than the shear effects of elastic medium, especially at low mode numbers. It is also observed that the effects of interlayer shear are pronounced at low mode numbers while it's the other way round for the effects of interlayer tensile-compressive. This study implies that for an accurate analysis of multi-layer graphene nanoribbons embedded in an elastic medium the tensile-compressive and shear effects of vdWs interactions between adjacent GNRs as well as elastic medium and GNRs must be contemplated simultaneously.

References

[1] Kordkheili SH, Moshrefzadeh-Sani H. Mechanical properties of double-layered graphene sheets. *Computational Materials Science* 2013; 69: 335-43.

[2] Allahyari E, Asgari M. Vibration Behavior of Nanocomposite Plate Reinforced by Pristine and Defective Graphene Sheets; an Analytical Approach. *International Journal of Engineering-Transactions A: Basics* 2018; 31(7): 1095-102.

[3] Shahsavari D, Karami B, Mansouri S. Shear buckling of single layer graphene sheets in hygrothermal environment resting on elastic foundation based on different nonlocal strain gradient theories. *European Journal of Mechanics-A/Solids* 2018; 67: 200-14.

[4] Shahsavari D, Karami B, Li L. Damped vibration of a graphene sheet using a higher-order nonlocal strain-gradient Kirchhoff plate model. *Comptes Rendus Mécanique* 2018; 346(12): 1216-32.

[5] Karami B, Shahsavari D, Li L. Hygrothermal wave propagation in viscoelastic graphene under in-plane magnetic field based on nonlocal strain gradient theory. *Physica E: Low-dimensional Systems and Nanostructures* 2018; 97: 317-27.

[6] Karami B, Shahsavari D, Janghorban M, Li L. Wave dispersion of mounted graphene with initial stress. *Thin-Walled Structures* 2018; 122: 102-11.

[7] Shahsavari D, Karami B, Janghorban M, Li L. Dynamic characteristics of viscoelastic nanoplates under moving load embedded within visco-Pasternak substrate and hygrothermal environment. *Materials Research Express* 2017; 4(8): 085013.

[8] Jabbarzadeh M, Sadeghian M. Nonlinear buckling of circular nano plates on elastic foundation. *International Journal of Engineering-Transactions B: Applications* 2016; 29(5): 697-705.

[9] Dastjerdi S, Jabbarzadeh M, Tahani M. Nonlinear bending analysis of sector graphene sheet embedded in elastic matrix based on nonlocal continuum mechanics. *International Journal of Engineering-Transactions B: Applications* 2015; 28(5): 802-11.

[10] Alibeigloo A. Three-dimensional free vibration analysis of multi-layered graphene sheets embedded in elastic matrix. *Journal of Vibration and Control* 2013; 19(16): 2357-71.
[11] Babaei H, Shahidi A. Vibration of quadrilateral embedded multilayered graphene sheets based on nonlocal continuum models using the Galerkin method. *Acta Mechanica Sinica* 2011; 27(6): 967-76.
[12] She G-L, Yuan F-G, Karami B, Ren Y-R, Xiao W-S. On nonlinear bending behavior of FG porous curved nanotubes. *International Journal of Engineering Science* 2019; 135: 58-74.
[13] Karami B, Shahsavari D, Karami M, Li L. Hygrothermal wave characteristic of nanobeam-type inhomogeneous materials with porosity under magnetic field. *Proceedings of the Institution of Mechanical Engineers, Part C: Journal of Mechanical Engineering Science* 2019; 233(6): 2149-69.
[14] Shi J, Ni Q, Lei X, Natsuki T. Nonlocal vibration of embedded double-layer graphene nanoribbons in in-phase and anti-phase modes. *Physica E: Low-dimensional Systems and Nanostructures* 2012; 44(7-8): 1136-41.
[15] Ansari R, Rajabiehfard R, Arash B. Nonlocal finite element model for vibrations of embedded multi-layered graphene sheets. *Computational Materials Science* 2010; 49(4): 831-8.
[16] Behfar K, Naghdabadi R. Nanoscale vibrational analysis of a multi-layered graphene sheet embedded in an elastic medium. *Composites science and technology* 2005; 65(7-8): 1159-64.
[17] Ansari R, Arash B, Rouhi H. Vibration characteristics of embedded multi-layered graphene sheets with different boundary conditions via nonlocal elasticity. *Composite Structures* 2011; 93(9): 2419-29.
[18] Nazemnezhad R, Shokrollahi H, Hosseini-Hashemi S. Sandwich beam model for free vibration analysis of bilayer graphene nanoribbons with interlayer shear effect. *Journal of Applied Physics* 2014; 115(17): 174303.
[19] Rokni H, Lu W. A continuum model for the static pull-in behavior of graphene nanoribbon electrostatic actuators with interlayer shear and surface energy effects. *Journal of Applied Physics* 2013; 113(15): 153512.
[20] Liu D, Chen W, Zhang C. Improved beam theory for multilayer graphene nanoribbons with interlayer shear effect. *Physics Letters A* 2013; 377(18): 1297-300.
[21] Mohammadimehr M, Mohammadi Najafabadi MM, Nasiri H, Rousta Navi B. Surface stress effects on the free vibration and bending analysis of the nonlocal single-layer graphene sheet embedded in an elastic medium using energy method. *Proceedings of the Institution of Mechanical Engineers, Part N: Journal of Nanomaterials, Nanoengineering and Nanosystems* 2016; 230(3): 148-60.
[22] Arani AG, Kolahchi R, Barzoki AAM, Mozdianfard MR, Farahani SMN. Elastic foundation effect on nonlinear thermo-vibration of embedded double-layered orthotropic graphene sheets using differential quadrature method. *Proceedings of the Institution of Mechanical Engineers, Part C: Journal of Mechanical Engineering Science* 2013; 227(4): 862-79.
[23] Shu C. **Differential quadrature and its application in engineering**: Springer Science & Business Media; 2012.
[24] Striz A, Wang X, Bert C. Harmonic differential quadrature method and applications to analysis of structural components. *Acta Mechanica* 1995; 111(1-2): 85-94.